

High Stability Measurement System for the Olimpo IR Calibration Source

M. Fesquet, P. Abbon, D. Yvon, A. Delbart

Abstract— A specific on-board electronic system has been developed for driving the infra red source calibration of the balloon-borne Olimpo. This system operates at ambient temperature, whereas the source is located on the 2K stage of the cryostat. This electronic system first generates a heating signal on the iridium strip of the source, and then monitors the source temperature stability by several measurements of an NbSi thermometer which is located under the source. Priority in the design was to achieve a high stability measurement, with low heating perturbations of the source, and with a large temperature range of the electronics. The design merges a modulated bias system, with a low noise voltage differential amplifier, and a digital acquisition. The whole system is driven by a microcontroller whose algorithm was optimized to minimize the noise perturbations. Electronic components have been selected for their large temperature operation range, and for their low temperature sensitivity. Moreover, the electronic system is designed to compensate the thermal deviation of the components. The system has been tested successfully with simulated and real IR source for several temperatures.

With 600pW of total sensor dissipation injected during 40ms, the measurement standard deviation achieved for the resistive value of a 10k Ω thermometer reaches 0,5 Ω (48ppm). Moreover the sensitivity of the electronic for the measurement is of 25ppm/ $^{\circ}$ C ranging from -60 $^{\circ}$ C to +20 $^{\circ}$ C, in agreement with the specifications.

I. INTRODUCTION

THE Olimpo balloon project [1] will observe the sky with 4 arrays of bolometers in the wavelength bands centered at 150, 220, 350 and 600GHz. The project is based on a 2.6 meter Cassegrain telescope mounted on a stratospheric balloon. The ground and in-flight calibration of the bolometric detectors is done by a sub-millimeter calibration lamp called “the Callamp” [2]. The main features of this device are the reproducibility and stability of the flux and a millisecond rise time. The Callamp is a thin sapphire plate containing on a side the radiative surface, and on the other side the heater and the

thermometer. The heater is a resistive line of iridium piloted by applying a controlled voltage, and the thermometer is a NbSi thin film whose behavior can be compared with that of a variable resistor. These two elements, the heater and the thermometer, are controlled by an electronic system which ensures the main feature of the Callamp. The description of this electronic system is the purpose of this article.

II. GENERAL DESCRIPTION

The view of the electronic board is presented on the Fig. 1. We chose to concentrate our efforts on the optimization of the electronic circuits and the programs, instead of choosing a system cooled and controlled in temperature.

It results that all the system is based on low cost classical components, some of them with military version to ensure the wide temperature range required.

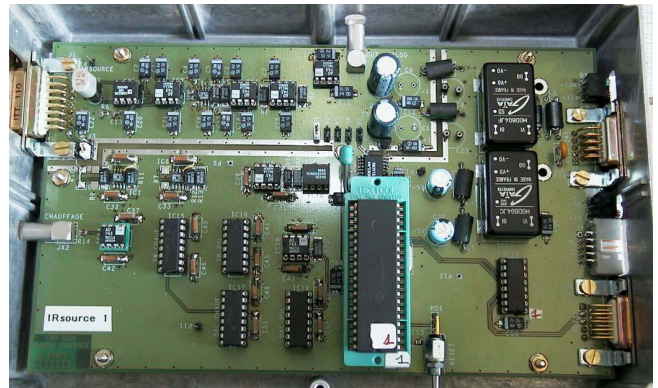


Fig. 1. The complete electronic board. The up-left part is dedicated to the analog zone, the lower-left part contains the digital circuits and the part on the right contains the alimentations and external communication devices.

The electronic system can be represented as a “black box” with several inputs and outputs, as shown in Fig. 2. The left box represents the Callamp containing the heating resistor, and the thermometer resistor connected to two 200k Ω resistors used to polarize the device.

The right box represents the electronic board that can be divided in three different systems: the heating system, the reading system and the control system.

-The purpose of the heating system is the generation of a variable voltage to be applied to the heating resistor.

- The purpose of the reading system is the production of the polarization current on the thermometer sensor, as well as the reading of the value of the terminal voltage of this sensor.

-At last, the purpose of the control system is to receive the order from the external PC, to pilot the heating and the reading

Manuscript received November 11, 2005.

This work was supported by the French government-funded technological research organization CEA.

Michel Fesquet is with the CEA-SACLAY, DSM/DAPNIA/SEDI/LDEF, 91191 Gif-Sur-Yvette Cedex FRANCE (telephone: 33 (0)169087939, e-mail: michel.fesquet@cea.fr).

Philippe Abbon is with the CEA-SACLAY, DSM/DAPNIA/SEDI/LDEF, 91191 Gif-Sur-Yvette Cedex FRANCE (telephone: 33 (0)169084927, e-mail: philippe.abbon@cea.fr).

Dominique Yvon is with the CEA-SACLAY, DSM/DAPNIA/SPP, 91191 Gif-Sur-Yvette Cedex FRANCE (telephone: 33 (0)169083625, e-mail: dominique.yvon@cea.fr).

Alain Delbart is with the CEA-SACLAY, DSM/DAPNIA/SEDI/LDEF, 91191 Gif-Sur-Yvette Cedex FRANCE (telephone: 33 (0)169083454, e-mail: alain.delbart@cea.fr).

systems, to calculate the value of the thermometer, and at the end, to send this value to the external PC.

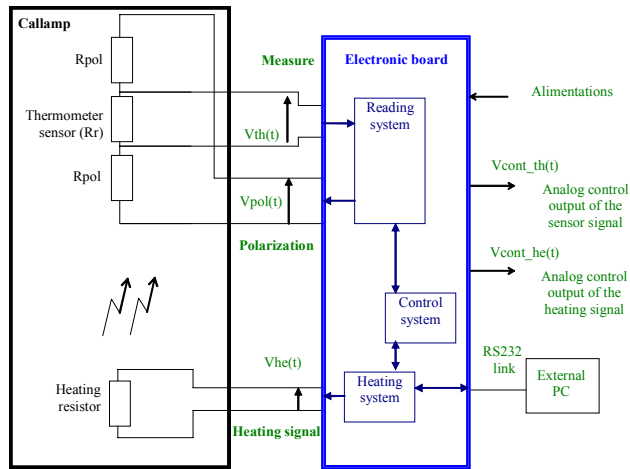


Fig. 2. General view of the electronic board with its context. This figure represents the Callamp interconnections and the electronic board control links.

When the user triggers a light pulse via the control system, the system performs a heat and measure cycle, as shown in Fig. 3. This cycle can be decomposed on the three following steps:

- Creation of a heating voltage $V_{he}(t)$ on a heating resistor, following a programmed scheme.
- During the application of this heating voltage, creation of a polarization voltage $V_{pol}(t)$ with two successive polarities, applied on the polarization resistors R_{pol} .
- During this polarization voltage step, reading of the resistance value of the thermometer sensor, and transmission of this value to an external PC by the RS232 link.

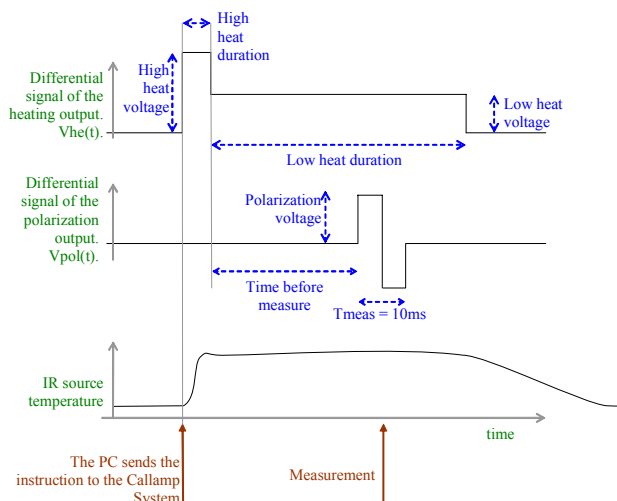


Fig. 3. Representation of heat and measure cycle. Upper, the signal represents the heating system, the intermediate signal represents the reading system and the bottom signal represents the deduced temperature of the Callamp source.

The variation of the biasing signal is essential for the stability of the reading system. This point will be developed further.

III. DESCRIPTION OF THE HEATING SYSTEM

This design is represented on Fig. 4. The heating signal is generated by a three position switch commuting the output signal to several voltages. The high and the low voltages are generated by a digital to analog converter commanded by the control system. The resulting signal is transmitted to the heating resistor by the means of a differential amplifier, and to the control output by the means of a common mode amplifier. With such a system, the produced signal can be the one represented on the upper part of Fig. 3.

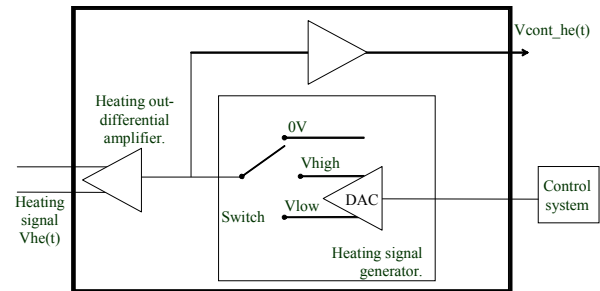


Fig. 4. Design of the heating system

IV. DESCRIPTION OF THE READING SYSTEM

The reading system is shown on Fig. 5.

The measurement occurs during the variation of the polarization voltage. This variation is achieved by varying a switch position between $0V$, $+V_{pol}$ and $-V_{pol}$, generated by a digital to analog converter (DAC). These operations are steered by the control system.

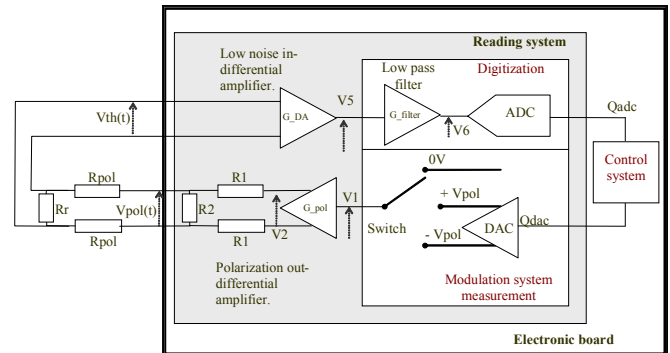


Fig. 5. Design of the reading system.

The measured $V_{th}(t)$ signal is amplified by the low noise differential amplifier, and then enters the digitization system. It goes then through a low pass filter, and enters an ADC component. This component makes N successive measurements of the voltage during the negative polarization ($-V_{pol}$), and then N successive measurements during the positive polarization ($+V_{pol}$). The control system collects the different values, and computes the mean value of the thermometer resistor. Those signals are represented on Fig. 6.

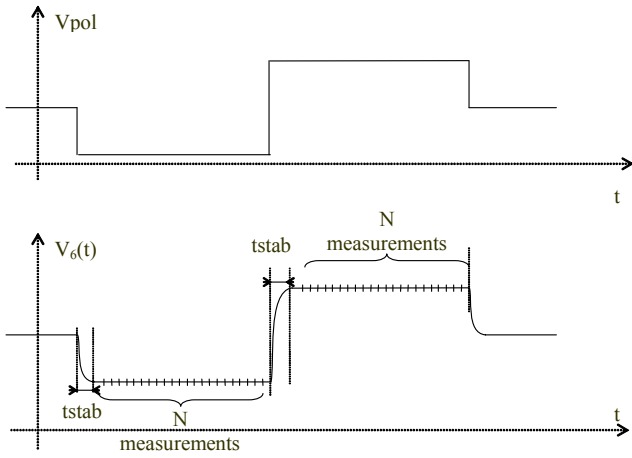


Fig. 6. Reading system process

The polarization-out differential amplifier consist of two low noise JFET polarized by two PNP cascode transistors. The varying drain current of the JFETs is measured by two operational amplifiers, and then subtracted by a last operational amplifier. The ratio of the system is controlled by a resistive feedback acting on the JFET source voltage. The output offset is cancelled by an active feedback injecting additional JFET drain current. Such a system shows a $2\text{nV}/\sqrt{\text{Hz}}$ voltage noise at 100Hz, with JFET operating at ambient temperatures.

V. DESCRIPTION OF THE CONTROL SYSTEM

The control system is based on a 8 bit CMOS Flash microcontroller. We decided to use a PIC16F877-20I/P device from Microchip Technology Inc [3]. This low cost device gathers some qualities sought for the system: 20MHz clock, serial port included (RS 232), several timers, 8K Flash program memory, 5 I/O digital ports, C code programming.

For the external control of the system, by serial interface (RS232), we developed a C library for the on-board system, and a LabVIEW interface for the lab experiment. With this external link, we can not only order a heating & reading cycle and recuperate the resistor value, but we can also change the parameter settings of the program. The C program realizes all the calculation to obtain the thermometer resistance value. The following lines will deal with this point.

The microcontroller receives a digital code from the ADC for each acquisition. Assuming that the arithmetic average of the digital code given is $data_1$ during the negative polarization and is $data_2$ during the positive polarization, we can evaluate the difference: $data_2 - data_1 = \Delta Q_{dac}$

The thermometer sensor value calculated by the control system is :

$$R_m = \frac{2 * \left(R_1 + R_{pol} * \left(1 + 2 * \frac{R_1}{R_2} \right) \right) * X * \Delta Q_{dac}}{1 - \left(1 + 2 * \frac{R_1}{R_2} \right) * X * \Delta Q_{dac}}$$

The X value is calculated with the electronic parameter of the system. With the notations from the Fig.4, we have:

$$X = \frac{V_{ref_adc}}{G_filter * G_DA * G_pol * 2 * V_{pol} * 2^{N_{dac}}}$$

With :

- V_{ref_adc} : the ADC reference voltage,
- N_{dac} : the ADC bits number,
- G_filter : the low pass filters gain,
- G_DA : the low noise differential amplifier gain,
- G_pol : the polarization amplifier gain,
- V_{pol} : the output DAC voltage.

Those equations suppose that we already know the applied polarization voltage value (V_{pol}). This value is calculated by the control system with the following formulas:

$$Q_{dac} = Ceil \left[\left(V_{pol_or} * \left(2 * \frac{R_1}{R_2} + 1 \right) * \frac{1}{G_pol} \right) * \frac{2^{N_{dac}}}{V_{ref_dac}} \right] \text{ and}$$

$$V_{pol} = Q_{dac} * \frac{V_{ref_dac}}{2^{N_{dac}}}$$

With:

- V_{pol_or} , the voltage polarization order received by the control system,
- V_{ref_dac} , the DAC reference voltage,
- N_{dac} : the DAC bits number.
- $Ceil [.]$ computes the smallest integer value greater than the argument.

The R_m value calculated by the control system can be compared to the real value. In Fig. 7, we can notice the simulated systematic error of measurement for a 10kΩ thermometer resistor value, and 200kΩ polarization resistors values.

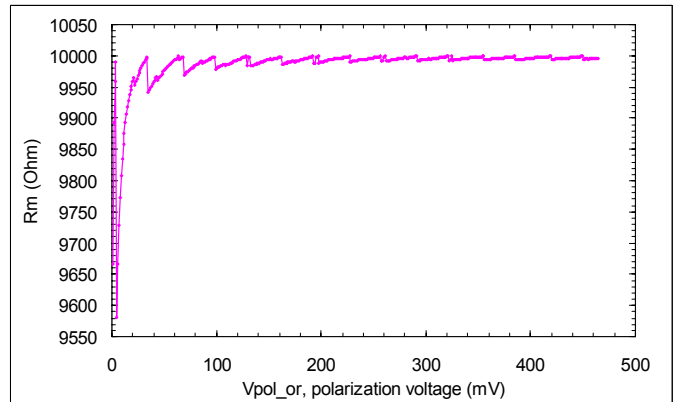


Fig. 7. Simulated measurement response of the system.

With the real system, a little variation of the polarization voltage (due to the noise) or of a component value will induce variations on the ADC value. The calculation of the effect on R_m (resistor value given by the CPU) of 1 bit error on the ADC value, gives the following expression: $\frac{\Delta R_m}{R_m} = \frac{\alpha}{V_{pol_or}}$, with α depending only on the components values, and V_{pol_or}

the user polarization order. Fig. 8 shows and confirms by experimental measurement the inverse dependence with V_{pol_or} .

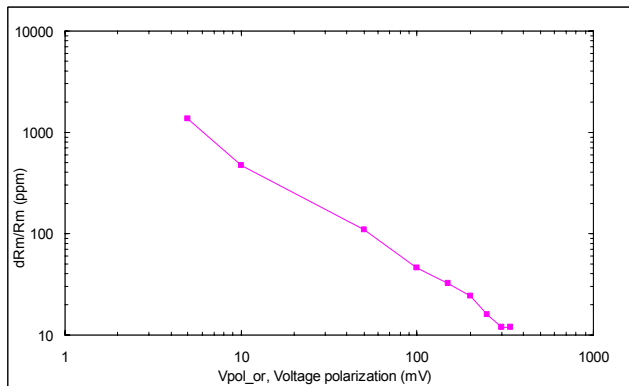


Fig. 8. Experimental validation of the law of dependence of the standard deviation measurement with the polarization order.

VI. IMPROVING THE FIDELITY OF THE MEASUREMENT

The improvement of the measurement fidelity can be done by four different ways:

1-Reducing the intrinsic noise of analogic components on the signal way: voltage reference, differential amplifier, DAC, filter, etc...

2-Increasing the number of measurements. The Fig. 9 shows an experimental variation of the standard deviation with the number of measurements. An approximation gives the following law of the standard deviation: $\frac{\sigma}{R} = 10 + \frac{250}{\sqrt{N}}$

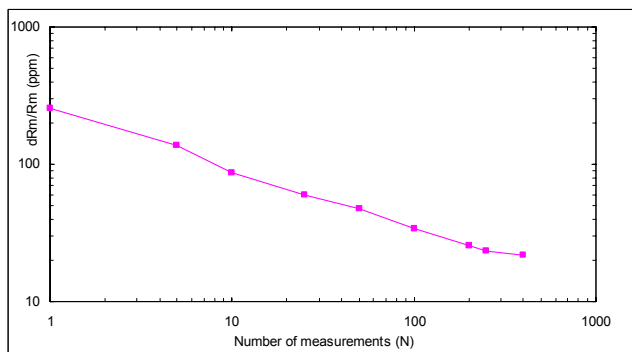


Fig. 9. Experimental effect of the number of measurements.

3-Calculating the optimal filter cut off frequency, once the measurement duration is fixed. The Fig. 10 shows the experimental effect of this frequency variation, and the existence of an optimal value.

This last point can be explained by considering that there are two contradictory effects. First, the growing of the cutoff frequency increases the noise participation; therefore it increases the standard deviation. Secondly, by growing the cutoff frequency, we reduce the t_{stab} value, and then increase the number N of measurement; therefore we reduce the standard deviation. This is the reason why we can observe a minimum on the curve, corresponding to the best group of parameter for a given total measurement duration.

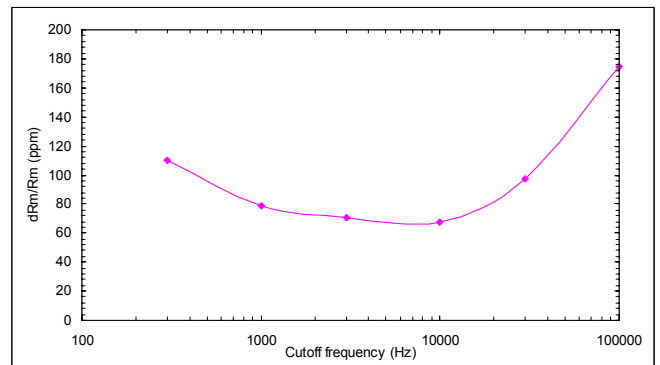


Fig. 10. Experimental optimization of the reading parameter with a fixed total duration of the measurement.

4- By software compensation of the components errors. Once the measurement is done, we can adjust in the calculus each value of component to the one directly measured. This is what Fig. 11 shows.

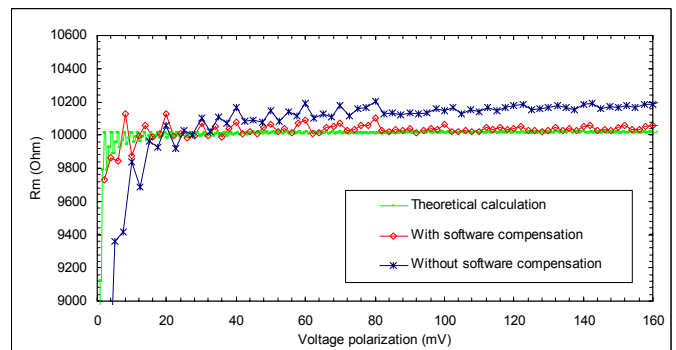


Fig. 11. Experimental validation of the software compensation of the components errors.

VII. GENERAL PERFORMANCES.

The behavior of the system with the temperature is presented in Fig. 12. We did several measurements with different values of the electronic board temperature, connected to a 10k Ω resistance placed at ambient temperature. That was done initially with an increasing temperature, then with a decreasing temperature. The vertical lines represent the noise at a fixed temperature. We can observe an hysteresis due to the two ways used for changing the temperature.

We achieve a reading temperature sensitivity of 25ppm/ $^{\circ}$ C.

We also can observe that the system was tested successfully from -60 $^{\circ}$ C to 20 $^{\circ}$ C

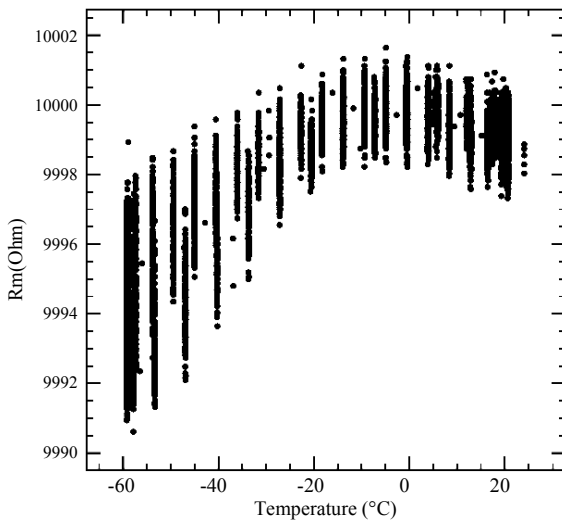


Fig. 12. Thermal behavior of the electronic board reading a 10kΩ resistance placed at ambient temperature.

Then, we evaluated the standard deviation of the measurement of a 10kΩ resistance at a stabilized temperature, this by varying the power injected into resistance to read. The result is presented on Fig. 13.

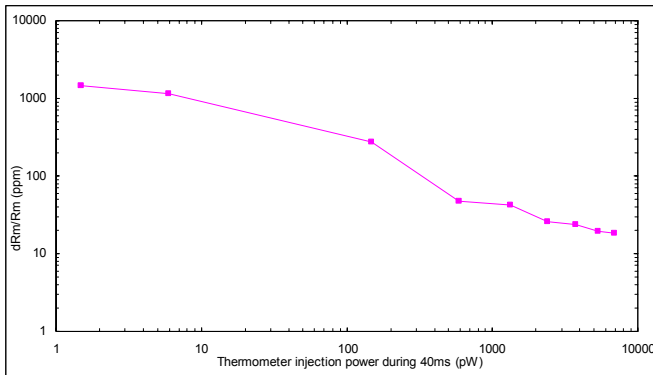


Fig. 13. Stability of measurement with the energy injected into the thermometer

As expected, the more resistance is heated, the more measurement is precise. For example, with 600pW injected during 40ms (24pJ), the standard deviation measurement of a 10kΩ thermometer is 0,5Ω (48ppm).

VIII. CONCLUSION

The system presented reaches the efficiency requested for the Olimpo Callamp. We made several events of the product to be ready for the payload integration and to explore and to improve the system in laboratory. It is also interesting to see that this product can be used each time that one wishes to read a resistive thermometer with a limited heating. The mean value of the resistor can be integrated on the system by adjusting the polarization components, and the program settings. The desired accuracy of measurement can be reached by adjusting the power injected in the thermometer or the duration of measurement. Lastly, the serial interface, the

existing C library and the LabVIEW interface make it a tool simple to use.

REFERENCES

- [1] S. Masi, P. Ade, P. de Bernardis, A. Boscaleri, M. De Petris, G. De Troia, M. Fabrini, M. Giacometti, A. Iacoangeli, L. Lamagna, A. Lange, P. Lubin, P. Mausekopf, A. Melchiorri, F. Melchiorri, F. Nati, L. Nati, A. Orlando, E. Pascale, F. Piacentini, M. Pierre, G. Polenta, Y. Rephaeli, G. Romeo and D. Yvon, "OLIMPO: A Few Arcmin Resolution Survey of the Sky at mm and Sub-mm Wavelengths", *Memorie della Società Astronomica Italiana*, Vol. 74, p. 96, n. 1, 2003
- [2] D. Yvon, J. P. Pansart, A. Delbart, C. Magneville, B. Mazeau, L. Dumoulin, L. Bergé, J. B. Juin, P. Abbon, M. Fesquet, P. Camus, "A millisecond-risetime sub-millimeter light source for lab tests and in flight bolometer calibration". Poster LTD11.
- [3] PIC16F873/4/6/7 Datasheet available on www.microchip.com